

EVALUATING THE DIRECT BLAST EFFECT IN MULTISTATIC SONAR NETWORKS USING MONTE CARLO SIMULATION

Mumtaz Karatas

Department of Industrial Engineering
Turkish Naval Academy
Tuzla, Istanbul, 34942, TURKEY

Emily Craparo

Department of Operations Research
Naval Postgraduate School
1411 Cunningham Road
Monterey, CA 93943, USA

ABSTRACT

Multistatic sonar networks generalize traditional sonar networks by allowing sources and receivers to occupy different physical locations. Although there are many advantages to a multistatic approach, there are also additional analytic challenges. One such challenge involves the *direct blast effect*, which can cause targets to go undetected even if they are within the nominal detection range of a sonar network.

Previous work has considered the problem of optimally provisioning and deploying a multistatic sonar network while neglecting to consider the blind zone. In this paper, we conduct Monte Carlo simulations to evaluate the impact of the direct blast effect on the performance of such a network. We find that for large pulse lengths, the direct blast effect can significantly decrease the performance of a multistatic network. Moreover, the optimal deployment policy can differ substantially when the direct blast effect is taken into account.

1 INTRODUCTION

Maritime warfare and exploration have long utilized sonar devices to conduct active sensing, and interest in this idea has experienced a renaissance in recent years due to advances in submarine technology (Lilley 2014). The basic operating principle behind sonar is that sound energy is emitted into the water, and the reflected echoes are used to detect, localize, and track targets of interest. In a traditional sonar system, sometimes called a *monostatic* system, a single device emits the initial sound burst (known as a “ping”) and listens for subsequent echoes. Recently, the idea has emerged of separating these two devices by emitting sound energy from a *source* and listening for echoes from a *receiver* at a different location. In most cases of interest, the distance between the source and receiver is large enough to be comparable to the distance to the potential target. The source of energy can be a ship with a hull-mounted sonar, a helicopter with a dipping sonar device, an explosive charge dropped by an aircraft, or an active sonobuoy. The receiver can be a passive ship-mounted device or a passive sonobuoy (Washburn 2010).

Multistatic systems have several advantages over monostatic systems. As described in (Cox 1989), one advantage lies in the covertness of the receiver devices. Because these devices do not emit sound energy and present a small sonar profile themselves, it is difficult for an enemy to locate and conduct countermeasures against them. Multistatic systems also enable multi-angle observations, which improve tracking accuracy. Furthermore, a multistatic approach facilitates multi-platform operations; for example, an airplane may deploy receiver sonobuoys while a surface ship or a dipping helicopter carries a source. A final advantage is cost: although sources can be expensive to procure and operate, receivers are generally relatively inexpensive (Amanipour and Olfat 2011, Washburn and Karatas 2015). Thus, while a monostatic sonar system must by definition contain equal numbers of sources and receivers, a multistatic

system may contain more receivers than sources and thus achieve similar sensing goals at a fraction of the cost of a monostatic system.

A multistatic system’s main disadvantage lies in its increased system complexity and the unusual coverage patterns determined by its transmission losses. For all sonar devices, both monostatic and multistatic, the probability of detecting a target via a direct return generally decreases as the target becomes more distant. For a single monostatic sensor, the detection probability is a simple function of the distance from the sonar device to the target. In a multistatic system, however, the probability of detecting a target with a particular source and receiver does not directly depend on the target’s distance from either one of these devices; rather, it depends on the product of the target’s distance from the source and its distance from the receiver (Cox 1989). As a result, for sensors and targets in the same 2-dimensional plane, the contours of constant detection probability take the form of Cassini ovals as shown in Figure 1.

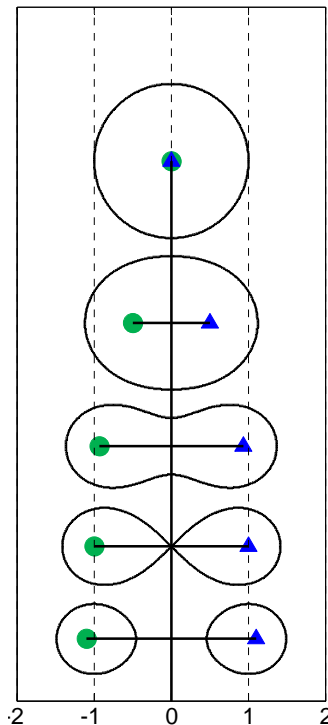


Figure 1: A family of Cassini ovals for various separation distances between the source and receiver. Receivers and sources are denoted by \blacktriangle and \bullet , respectively. From Craparo and Karatas (2015). Under a definite range (“cookie cutter”) sensor model, a target is detected if it lies within the detection region (Cassini oval) for some source and receiver, and otherwise it is not detected.

To complicate matters further, there also exists an ellipsoidal “blind zone” (also known as a “dead zone”) between the source and receiver in which detection probability plummets (Fewell and Ozols 2011). This blind zone exists because within this region, the reflected sound from the target arrives at the receiver at nearly the same time as the original ping. This phenomenon, known as the *direct blast effect*, causes the reflected signal to be obscured, drastically reducing detection probability (Cox 1989).

Various recent studies consider multistatic sonar network performance in the context of a definite range (“cookie cutter”) sensor model in which a target is detected if it lies within the detection region for some source and receiver, and otherwise it is not detected (Craparo and Karatas 2015, Washburn and Karatas 2015). These works consider targets and sensors that exist in the same 2-dimensional plane, although most results generalize to three dimensions with little difficulty. Washburn (2010) and

Washburn and Karatas (2015) consider a field of randomly-placed sources and receivers and develop a simple analytic theory for predicting the coverage of the network, ignoring the direct blast effect. Although they do not directly account for the direct blast effect, the authors provide two theorems that offer lower bounds on the detection performance of multistatic systems, and Washburn (2010) confirms the bounds by simulation experiments. The analytical results in their work contribute the multistatic search theory by allowing average detection probability to be predicted for a particular sensor mix deployed randomly; this result can then be used as a foundation to study pattern optimization and cost/effectiveness (i.e. how many sensors to buy and how to deploy them). However, because these studies do not account for the direct blast effect, their applicability is limited. Thus, in this study, our main ambition is to analyze the impact of direct blast effect using simulation. We conduct Monte Carlo simulations to compare the predicted and actual performance of multistatic sonar networks in which sensors are placed randomly, as in Washburn and Karatas (2015), while accounting for the direct blast effect. Although our motivation comes primarily from underwater detection systems, many of our simulation results are generalizable to radar or geolocation systems.

The organization of the paper is as follows: Section 2 provides the mathematical details involved in modeling multistatic sonar networks, including the direct blast effect. Section 3 provides the details of our simulation model and the numerical results it generates. Finally, Section 4 summarizes our results and provides our conclusions.

2 MULTISTATIC THEORY

2.1 Random Multistatic Networks

Washburn and Karatas (2015) consider a multistatic network containing a set of sources, S , and receivers, R , randomly deployed in a square region of area A . They show that for large A , coverage can be maximized by concentrating the sensors in a square sub-region of area A' which is contained in A and whose center coincides with that of A . More specifically, the authors define an “effort density” parameter

$y = \frac{2\pi\rho^2 \sqrt{|S||R|}}{A}$, where ρ is the equivalent monostatic detection range (i.e., the detection range when source and receiver are co-located) and compute the optimal A'/A ratio as:

$$\frac{A'}{A} = \begin{cases} \frac{y}{1.1} & \text{if } y \leq 1.1 \\ 1 & \text{if } y > 1.1 \end{cases} . \quad (1)$$

They also show that the resulting equivalent area covered will be:

$$C = 0.8\pi\rho^2 \sqrt{|S||R|} . \quad (2)$$

These analytical formulas do not consider the direct blast effect, which we now describe in more detail.

2.2 Direct Blast Effect

The blind zone for a particular source and receiver is the set of locations from which the echo from a target would arrive at the receiver at nearly the same time as the original ping from the source. Thus, the size of the blind zone is affected by the duration of the original ping, with longer pings resulting in larger blind zones. In practice, an operator will choose a ping duration that is appropriate for the expected distance of the target, typically from among a finite set of possible ping durations available on a particular sonar device.

To understand the geometry of the blind zone, consider a monostatic sensor whose ping lasts τ seconds and travels at a speed of v m/s, and assume that a target is not detected if any portion of its echo reaches the receiver while the original ping is still being received. Suppose that a ping occurs during time interval $[0, \tau]$, and a target is located at distance d from the sonar device. The echo from the target will reach the device during time interval $\left[\frac{2d}{v}, \frac{2d}{v} + \tau\right]$; thus, detection will not occur if $\frac{2d}{v} < \tau$; or,

equivalently, if the target is located inside an open disk-shaped region with radius $r_b = \frac{v\tau}{2}$ centered at the

sonar device, i.e., if $d < \frac{v\tau}{2}$. The parameter r_b is known as the *pulse length*, and it is the distance a ping travels during time τ . For the multistatic case, the blind zone takes on an elliptical shape. To see this,

consider a single source, receiver, and target, and let $d_{s,t}$, $d_{t,r}$, and $d_{s,r}$ denote the source-target, target-receiver and source-receiver distances, respectively. If a ping begins at time 0, the receiver will receive the ping during time window $\left[\frac{d_{s,r}}{v}, \frac{d_{s,r}}{v} + \tau\right]$, and it will receive the target echo during time window

$\left[\frac{d_{s,t} + d_{t,r}}{v}, \frac{d_{s,t} + d_{t,r}}{v} + \tau\right]$. Thus, detection will not occur if $\frac{d_{s,t} + d_{t,r}}{v} < \frac{d_{s,r}}{v} + \tau$, or, equivalently, if

$$d_{s,t} + d_{t,r} < d_{s,r} + 2r_b. \quad (3)$$

To study the impact of the blind zone on detection contours, we define a dimensionless parameter $k = \frac{r_b}{\rho}$ that reflects the relationship between the pulse length r_b and the equivalent monostatic detection range ρ . A long pulse length (and high value of k) reflects a ping of relatively long duration, which results in a larger loss of coverage due to the direct blast effect than a ping of short duration. A value of $k=1$ reflects an extreme situation in which the ping duration is so long that all targets within the detection range of a monostatic sensor go undetected due to the direct blast effect. Figure 2 depicts the blind zones for various source-receiver pairs for $k=0.01, 0.05, 0.1$ and 0.2 . Clearly, larger values of k result in larger blind zones. However, it is also interesting to note the impact of $d_{s,r}$: as $d_{s,r}$ increases, we see that the blind zone increases in size and thickness, even as the size of the nominal detection region decreases. This interaction between k and $d_{s,r}$ is quite difficult to model analytically, and this complexity is exacerbated when multiple sources and receivers are present. Thus, we now turn our attention to a simulation study of the direct blast effect.

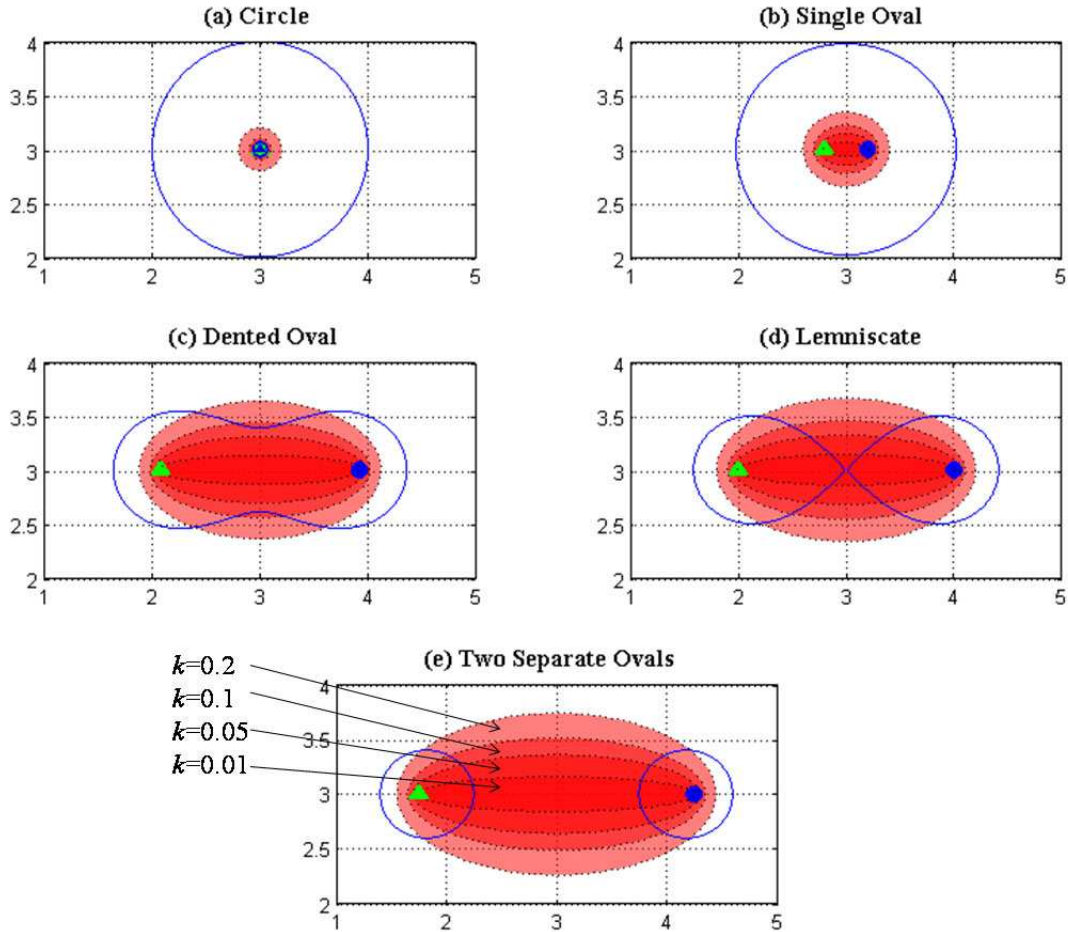


Figure 2: Direct blast zones for $k=0.01, 0.05, 0.1$ and 0.2 when the Cassini oval is in the form of (a) a circle (reflecting a monostatic sensor) (b) a single oval, (c) a dented oval, (d) a lemniscate, and (e) two disjoint ovals.

3 SIMULATION OF THE DIRECT BLAST EFFECT IN MULTISTATIC NETWORKS

We first perform computational experiments to determine the sub-region area A' that maximizes the coverage when direct blast effect is considered for different values of k , and we compare it with the area predicted by Equation (1). Then we evaluate the performance of various multistatic networks in terms of coverage, and we compare the results with a situation in which the direct blast effect does not occur. The pseudocode for our simulations appears in Figure 3.

We use MATLAB®2013a to randomly generate 10^3 BLINDZONE instances for each setup we consider. For our experiments, we generate 500 target locations uniformly at random in a 120×120 unit 2-dimensional area A . We consider varying numbers of sources and receivers ranging from $(|S|, |R|) = (5, 5)$ to $(|S|, |R|) = (25, 25)$. For each sensor mix (i.e., each value of $|S|$ and $|R|$), we run the simulation for different sub-region areas A' . In particular, we consider $A' = n^2$ for $n = 20, 24, 28, \dots, 100$ units, and we compute the coverage ratio for each A' . We perform these simulations for $k = 0, 0.01, 0.1, \text{ and } 0.2$, and we fix ρ at 10 units.

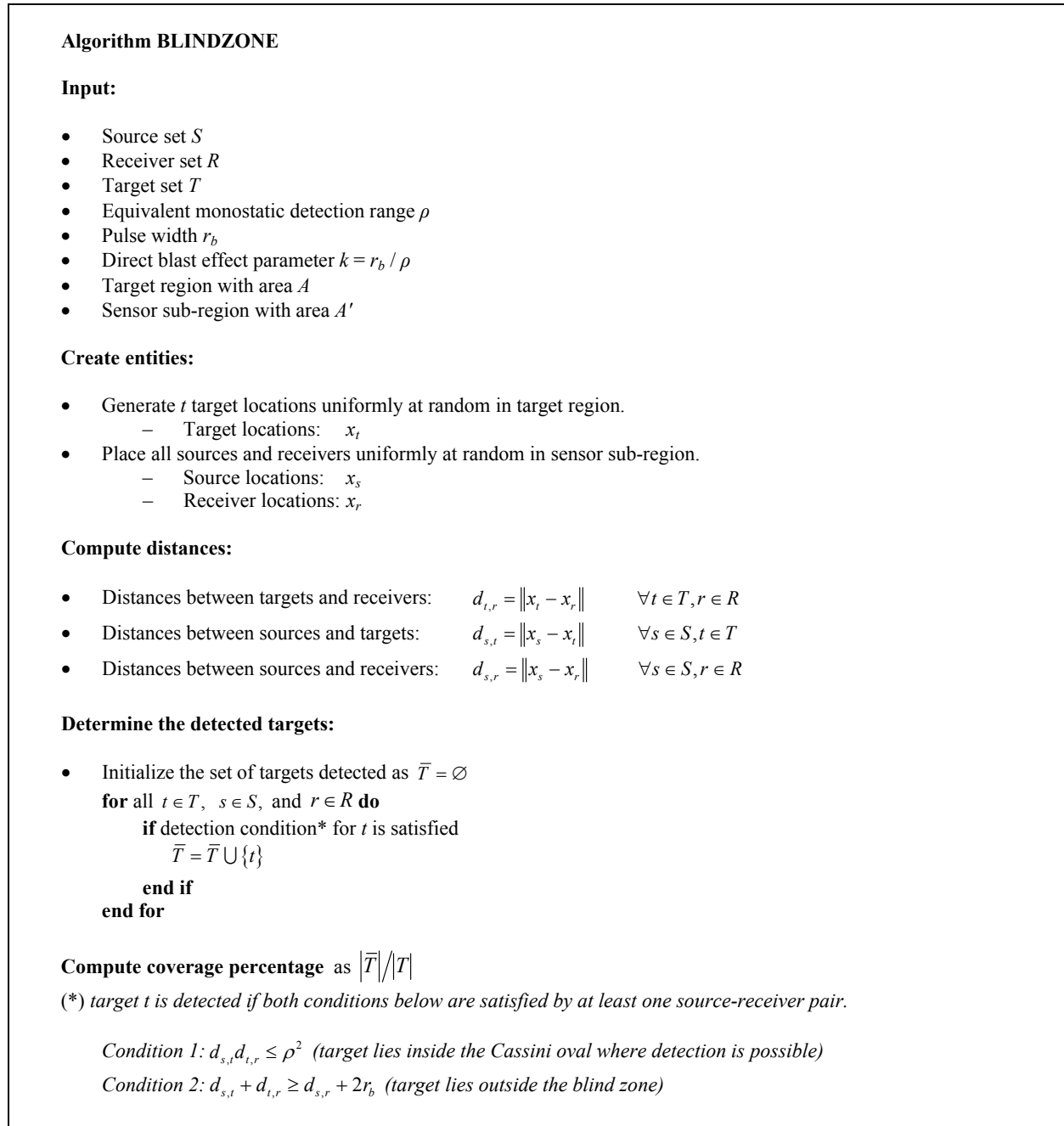


Figure 3: Pseudo-code for evaluating the performance of randomly-deployed multistatic networks while accounting for the blind zone.

Figure 4 shows a sample replication of a simulation experiment. All targets that lie within the detection zone (i.e., inside the nominal detection region and outside the blind zone) of at least one source-receiver pair are detected. Note that some targets that lie inside a blind zone (shaded area) of a certain source-receiver pair are detected since they lie inside the detection zone of some other source-receiver pair.

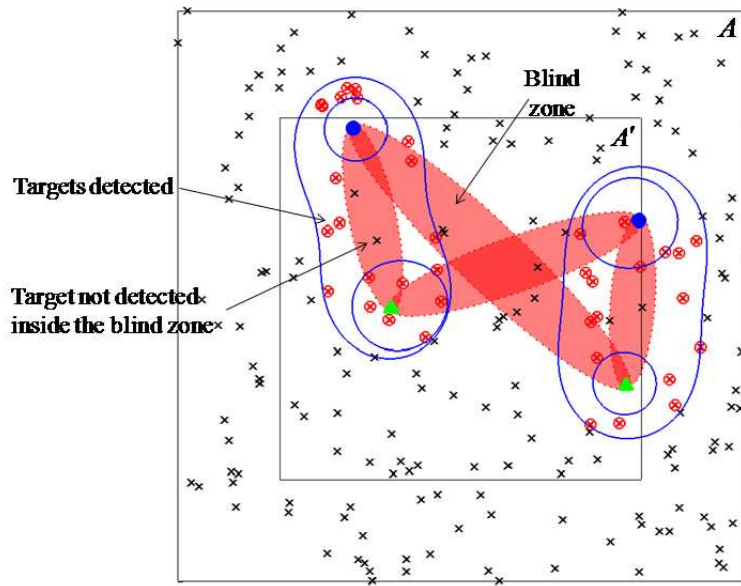


Figure 4: Example replication of our simulation experiment to measure coverage percentage. Receivers are denoted by \blacktriangle , sources are denoted by \bullet , detected targets are denoted by \otimes and undetected targets are denoted by \times .

Table 1 summarizes the results of our first set of computational experiments, and Figures 5 and 6 depict them graphically. As these results indicate, the qualitative behavior of Equation (1) is preserved when the blind zone is taken into account. In particular, larger values for $|S|$ and $|R|$ result in larger optimal (A'/A) ratios. However, we note that the blind zone can result in significantly different optimal (A'/A) ratios than are predicted by Equation (1). Indeed, for $k=0.2$, the optimal (A'/A) ratio is approximately half that predicted by Equation (1). Moreover, as Figure 6 indicates, a suboptimal (A'/A) ratio can result in substantially inferior coverage compared to an optimal (A'/A) ratio. Thus, the blind zone is an important practical consideration that should be taken into account by multistatic sonar operators.

Table 1: Optimal (A'/A) ratio and respective coverage percentage as reported by algorithm BLINDZONE for different values of $|S|$, $|R|$, and k averaged over 10^3 randomly-generated problem instances for each sensor mix. Values for $k=0$ are computed using Equation (1).

$ S $	5	5	5	5	5	10	10	10	10	10	15	15	15	15	15	20	20	20	20	20	25	25	25	25	25
$ R $	5	10	15	20	25	5	10	15	20	25	5	10	15	20	25	5	10	15	20	25	5	10	15	20	25
Optimal (A'/A) Ratio ($A = 10,000 \text{ unit}^2$)																									
$k=0$	0.29	0.40	0.49	0.57	0.64	0.40	0.57	0.70	0.81	0.90	0.49	0.70	0.86	0.99	1.00	0.57	0.81	0.99	1.00	1.00	0.64	0.90	1.00	1.00	1.00
$k=0.01$	0.23	0.31	0.36	0.46	0.41	0.27	0.46	0.58	0.71	0.71	0.36	0.58	0.77	0.92	0.92	0.46	0.64	0.77	1.00	1.00	0.52	0.71	0.92	1.00	1.00
$k=0.1$	0.16	0.27	0.31	0.36	0.36	0.23	0.36	0.46	0.52	0.64	0.31	0.52	0.64	0.71	0.85	0.31	0.58	0.71	0.92	0.85	0.41	0.64	0.77	0.92	0.92
$k=0.2$	0.13	0.19	0.27	0.27	0.31	0.23	0.31	0.36	0.46	0.52	0.23	0.36	0.46	0.58	0.58	0.31	0.41	0.58	0.64	0.71	0.36	0.52	0.64	0.71	0.85
Coverage % for Optimal (A'/A) Ratio ($A = 10,000 \text{ unit}^2$)																									
$k=0$	9%	12%	15%	17%	19%	12%	17%	21%	24%	27%	15%	21%	25%	29%	33%	17%	24%	29%	34%	38%	19%	27%	33%	38%	42%
$k=0.01$	8%	12%	14%	16%	18%	12%	17%	20%	23%	26%	14%	20%	25%	29%	32%	17%	23%	29%	33%	37%	18%	26%	32%	37%	41%
$k=0.1$	8%	11%	13%	15%	16%	11%	15%	18%	21%	24%	13%	18%	22%	26%	29%	15%	21%	26%	30%	34%	16%	24%	29%	34%	37%
$k=0.2$	7%	9%	11%	13%	14%	9%	13%	16%	19%	21%	11%	16%	20%	23%	26%	13%	19%	23%	27%	30%	14%	21%	26%	30%	33%

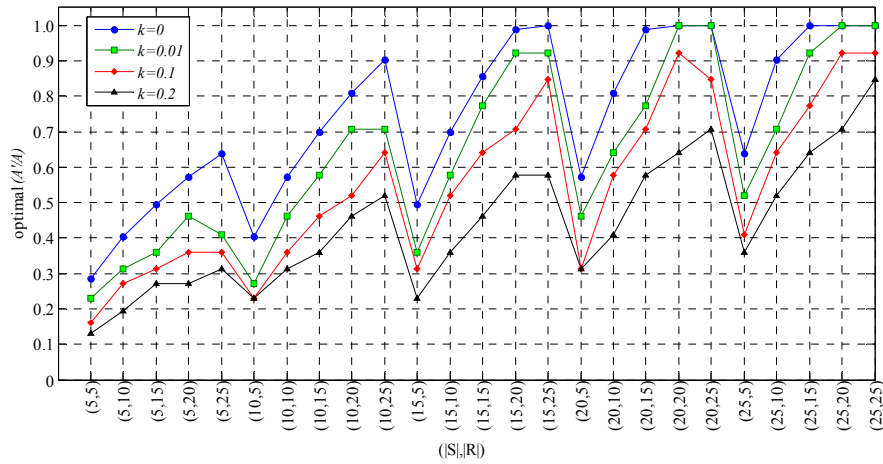


Figure 5: Optimal (A/A) ratios for various sensor mixes. Values for $k=0$ are computed using Equation (1). Values for $k=0.01, 0.1$ and 0.2 are those ratios that perform best, on average, over the 10^3 trials.

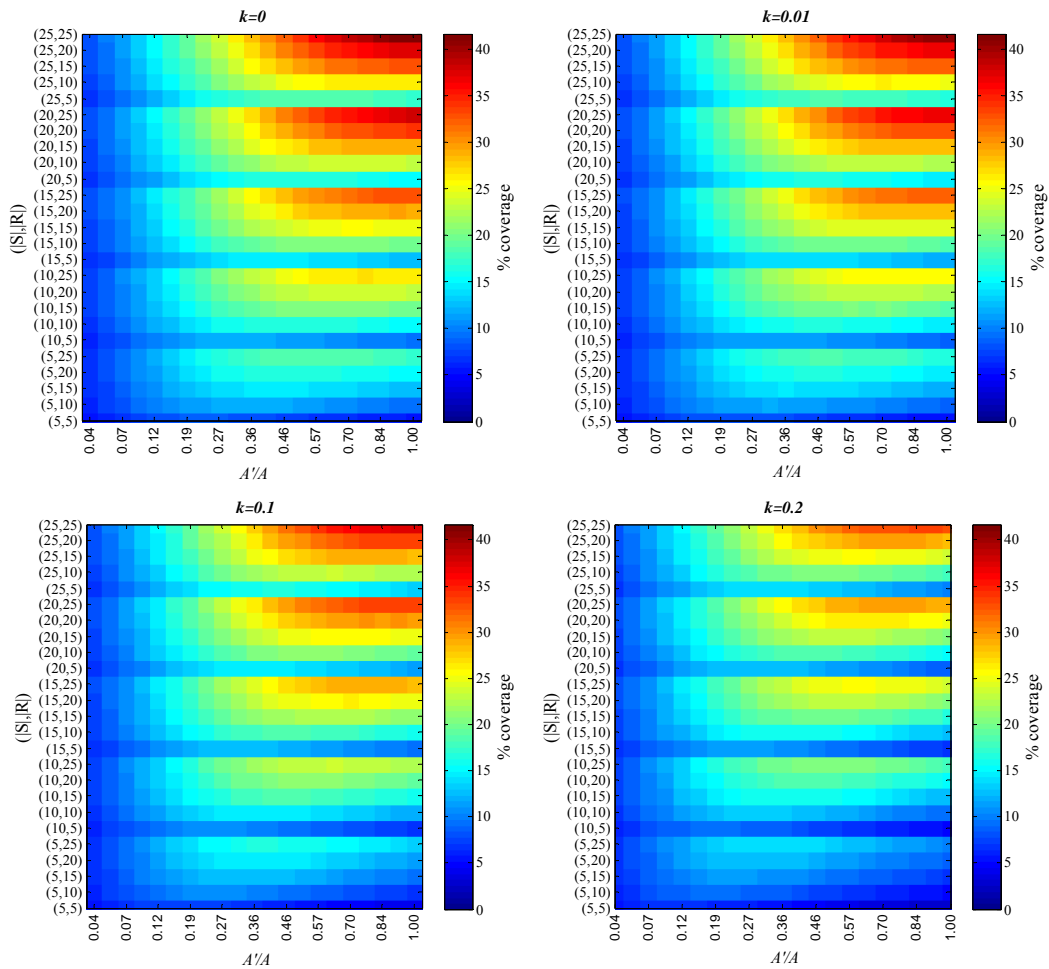


Figure 6: Coverage percentages for various sensor mixes and A/A ratios (higher coverage is better). Values for $k=0, 0.01, 0.1$ and 0.2 represent average quantities over the 10^3 trials.

In our second group of simulations, we study the coverage performance for a fixed target region of size $A=6400$ units and a fixed sensor sub-region of size $A'=3600$ units. Once again we consider sensor mixes of $(|S|,|R|)=(5,5), (5,10), \dots, (25,25)$ as shown on the vertical axis of Figure 6, and we consider direct blast effect parameters $k=0, 0.01, 0.1, \text{ and } 0.2$. We generate 10^3 replications for each sensor mix; in each replication we generate 500 target locations uniformly at random in the target region and generate source and receiver locations uniformly at random in the sensor sub-region. We compute the coverage percentages for each instance, where ρ is fixed at 10 units. These performance results are shown graphically in Figures 7 and 8. Figure 7 depicts the average coverage percentage for the 10^3 replications for each sensor mix; note that the upper left portion of Figure 7 corresponds to a situation in which $k=0$, i.e., the direct blast effect does not occur. Comparing the coverage achieved for various values of k , we see a marked decrease in coverage as k increases. This loss is highlighted in Figure 8, which shows the loss in nominal coverage percentage for various values of k . That is, if a particular sensor mix achieves expected coverage c_0 when $k=0$ and c_k for some $k>0$, we compute the loss in nominal coverage percentage as $\frac{c_0 - c_k}{c_0}$ and present this in Figure 8.

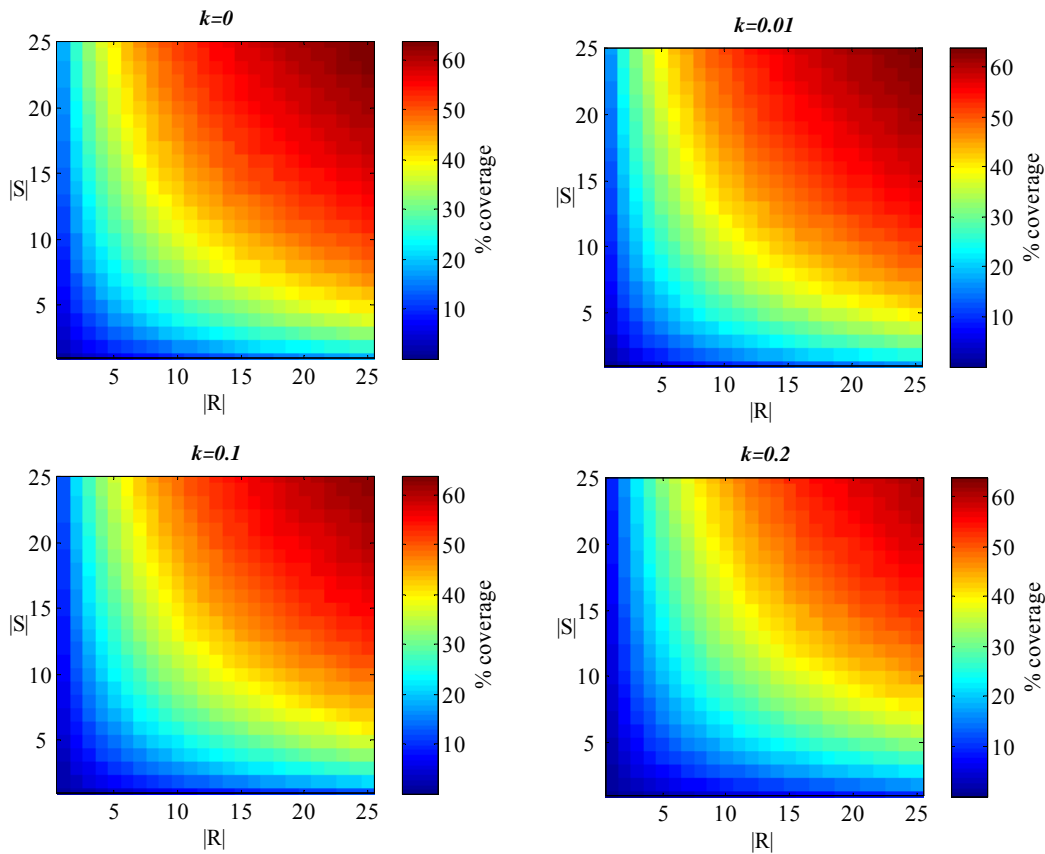


Figure 7: Average coverage percentages over the 10^3 trials for various sensor mixes and for $k=0, 0.01, 0.1$ and 0.2 (higher coverage is better).

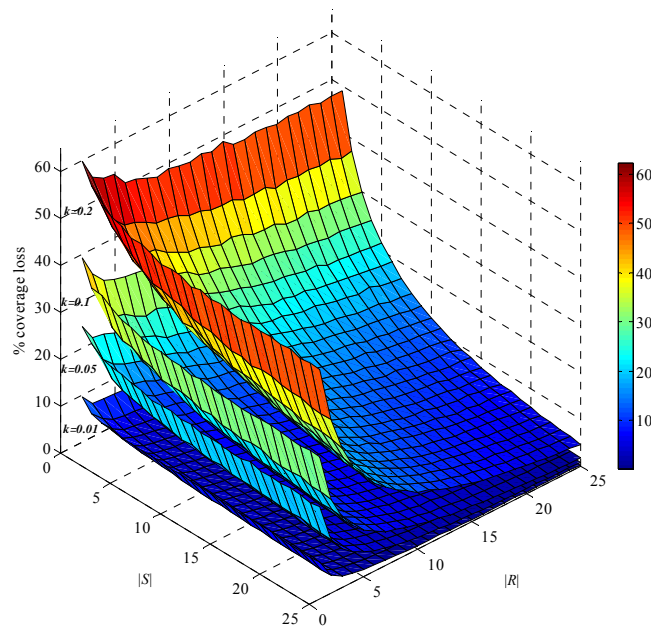


Figure 8: Average coverage loss percentages over the 10^3 trials for various sensor mixes and for $k=0.01$, 0.05, 0.1 and 0.2 (lower coverage loss is better). Note that large values for k can result in significant coverage loss, particularly when only a small number of sources or receivers is available.

As expected, more generous sensor mixes (i.e., large $|S|$ and $|R|$) result in greater coverage. However, we also see that more impoverished sensor mixes (i.e., small $|S|$ and $|R|$) not only have lower nominal coverage, but also greater loss of coverage as k increases. This phenomenon occurs because a larger number of sensors provides more opportunities for a target to be covered by the nominal detection region of more than one source and receiver. Thus, if the target happens to be in the blind zone for one source and receiver pair, it may be detected by a different source and receiver whose blind zone lies elsewhere. There is less opportunity for this compensation mechanism to occur when $|S|$ and $|R|$ are low. Thus, we conclude that the direct blast effect is a particularly important consideration when deploying a small number of sensors.

4 CONCLUSIONS AND FUTURE WORK

Our computational experiments indicate that the blind zone is an important consideration when deploying multistatic sonar networks. In particular, the blind zone impacts both the optimal area over which a randomly-deployed sonar network should be fielded, as well as the coverage that should be expected given such a deployment.

Although we have only considered randomly-deployed multistatic networks in this paper, there also exist algorithms for optimally placing multistatic sensors, neglecting the blind zone (Craparo and Karatas 2015, Kuhn 2014, Hof 2015). One area for further research is on modification of these algorithms to account for the blind zone. Additionally, although we only considered stationary targets, many interesting targets are, in fact, mobile. A future simulation study may consider mobile targets that traverse the target region; it is possible that detection of such targets might be less susceptible to the effects of the blind zone, since it is often necessary to pass through some part of the detection zone before reaching the blind zone. Finally, although we have varied k and ρ separately, in practice they are related. Future work may relate k and ρ to the ping duration, and study the problem of determining an optimal ping duration.

ACKNOWLEDGMENTS

The authors thank Prof. Alan Washburn for many insightful discussions. Dr. Craparo is funded by the Office of Naval Research (ONR).

REFERENCES

- Amanipour, V., and A. Olfat. 2011. "CFAR Detection for Multistatic Radar." *Signal Processing* 91(1): 28-37.
- Cox, H. 1989. "Fundamentals of Bistatic Active Sonar." *Underwater Acoustic Data Processing*, edited by Y. Chan, 3–24. Kluwer.
- Craparo, E. and M. Karatas. 2015. "Optimal Sensor Placement for Point Coverage in Active Multistatic Sonar Networks," submitted for review.
- Fewell, M.P., and S. Ozols. 2011. "Simple Detection-Performance Analysis of Multistatic Sonar for Anti-submarine Warfare." Technical report DSTO-TR-2562, Defence Science and Technology Organisation, Edinburgh, South Australia.
- Hof, C. 2015. "Optimization of Source and Receiver Placement in Multistatic Sonar Environments." Master's thesis, Naval Postgraduate School, Monterey, CA.
- Kuhn, T. U. 2014. "Optimal Sensor Placement in Active Multistatic Sonar Networks." Master's thesis, Naval Postgraduate School, Monterey, CA.
- Lilley, R. 2014. "Recapture Wide-area Anti-submarine Warfare." *Proceedings Magazine* 140/6/1336. U.S.Naval Institute, 44.
- Washburn, A. R. 2010. "A Multistatic Sonobuoy Theory." Technical Report NPS-OR-10-005, Naval Postgraduate School, Monterey, California.
- Washburn, A.R. and M. Karatas. 2015. "Multistatic Search Theory." *Military Operations Research* 20(1): 21-38.

AUTHOR BIOGRAPHIES

MUMTAZ KARATAS graduated from the Turkish Naval Academy in 2001. He received his MS degree in Industrial & Operations Engineering from University of Michigan and his Ph.D. degree in Industrial Engineering from Kocaeli University. He spent two years at the Naval Postgraduate School as a visiting researcher and postdoctoral fellow between 2011 and 2013. He is currently an Assistant Professor in the Industrial Engineering Department at the Turkish Naval Academy. His current research areas include optimization and military operations research. His email address is mkaratas@dho.edu.tr.

EMILY M. CRAPARO is an Assistant Professor of Operations Research at the Naval Postgraduate School. She obtained her Ph.D., S.M., and S.B. in Aeronautics & Astronautics at the Massachusetts Institute of Technology. Prior to joining the Operations Research faculty at the Naval Postgraduate School, she completed a National Research Council Postdoctoral Fellowship in the same department. Her research areas include mathematical modeling, optimization, and military applications. Her email address is emcrapar@nps.edu.